Far-field flow and drift due to particles and organisms in density-stratified fluids

Vaseem A. Shaik and Arezoo M. Ardekani ⬡[*]

School of Mechanical Engineering, Purdue University, West Lafayette, Indiana 47907, USA

In the limit of small inertia, stratification, and advection of density, Ardekani and Stocker [Phys. Rev. Lett. **105**, 084502 (2010)] derived the flow due to a point-force and force-dipole placed in a linearly density-stratified fluid. In this limit, these flows also represent the far-field flow due to a towed particle and a neutrally buoyant swimming organism in a stratified fluid. Here, we derive these two far-field flows in the limit of small inertia, stratification but at large advection of density. In both these limits, the flow in a stratified fluid decays rapidly and has closed streamlines but certain symmetries present at small advection are lost at large advection. To illustrate the application of these flows, we use them to calculate the drift induced by a towed drop and a swimming organism, as a means to quantify the mixing caused by them. The drift induced in a stratified fluid is less than that in the homogeneous fluid. A towed drop induces a large drift relative to its own volume at small advection while it induces at least an order of magnitude smaller drift at large advection. On the other hand, a swimming organism induces a large partial drift as compared with its own volume irrespective of the magnitude of advection, unless the stresslet exerted by the swimmer is small. These results are useful in understanding the stratification effects on the drift-based contributions to mixing.

I. INTRODUCTION

Density stratification, in its natural setting, occurs in the oceans, lakes, or ponds due to the variation of the temperature or the salt concentration with height. The stratification alters the settling rates of organic matter in the ocean which affects the carbon flux as well as the nutrient transport from the surface to the bottom of the ocean [1–6]. Sharp density changes inhibit the motion of several swimming organisms [7–10] and are also responsible for the formation of the frequently observed algal blooms [11]. Due to the inherent nature of the stratification to suppress the vertical motion, it is expected that the stratification reduces the mixing caused by the settling particles and swimming organisms [12–14]; however, a consistent analysis of this argument is still lacking.

A decade ago, Ardekani and Stocker [15] reported the flow due to a point force and a force-dipole in a density-stratified fluid in the limit of small inertia, stratification and advective transport rate of density. These point force singularity solutions paved the way towards calculating the mixing caused by a settling particle or a swimming organism in a stratified fluid. For instance, Wagner *et al.* [16] quantified the mixing through the mixing efficiency—the ratio of the rate of creation of gravitational potential energy to the rate of work done on the fluid—and found that the mixing efficiency of a settling particle and a neutrally buoyant swimming organism scales as a/l and $(a/l)^3$, respectively, where a is the characteristic size of the particle (or the organism), $l = (\nu\kappa/N^2)^{1/4}$ is the intrinsic length scale for stratified flows, ν is the kinematic viscosity, κ is the diffusivity, and N is the buoyancy frequency (or Brunt-Vaisala frequency). For weak stratifications,

$a/l \ll 1$, this means that the settling particle and the swimming organism are only 10% and 0.1% efficient in mixing their surroundings and this leads to the conclusion that the swimming microorganisms are incapable of mixing their surroundings or the ocean. Just like in the homogeneous fluids, the flow due to a point-force and a force-dipole in stratified fluids still represent the flow far away from a settling particle and a neutrally buoyant swimming organism. The knowledge of this far-field flow enables us to find the induced drift, i.e., the volume of the displaced fluid [17]. The calculation of drift allows us to better understand the mixing caused by the settling particles or the swimming organisms [18,19]. We found that a rising drop or a settling particle in a stratified fluid induces a large but finite drift volume unlike an infinite drift volume induced in a homogeneous fluid [17]. This means that the settling organic matter in the stratified ocean can significantly mix its surroundings but not as much as that in homogeneous fluids.

The analysis in the density-stratified fluids is far from complete. Most works mentioned in the previous paragraph are valid in the limit of low Péclet number (Pe), where the Péclet number is the ratio of the advection to the diffusion of the density. We expect a similar analytical solution for the flow and density fields at the other extreme values of Péclet number, namely high Pe, to be helpful in better understanding the transport of particles and organisms in stratified fluids. A similar flow far from a settling sphere was derived earlier in the Fourier space [20], but this flow was directly used to determine the drag enhancement on the sphere without any attention to the details of the flow field. To illustrate one of the applications of this flow field, we use it to find the drift induced by a towed drop or particle in a stratified fluid at high Pe. As for the neutrally buoyant swimming organism, we use the flow far from the organism both at low Pe (Stratlet-dipole

---

[*]ardekani@purdue.edu

[15]) and at high Pe (derived here) to find the drift induced by the organism at the respective Pe. Hence, we close the gap in the literature where the focus was on finding the flow far from a settling sphere and a swimming organism at low Pe, and the drift induced by a rising drop or particle at low Pe by generalizing the former calculations to high Pe, and also by finding the drift induced by a rising drop or particle as well as a swimming organism at both low and high Pe.

Few numerical or theoretical studies were performed in the past to determine the swimming speed of a spherical squirmer or Taylor's swimming sheet in a stratified fluid at finite inertia and stratification strength and the mixing caused by a single or a dilute suspension of model swimmers [9,10,21,22].

List and later Ardekani and Stocker reported the existence of a length scale $l = (\nu \kappa / N^2)^{1/4}$ in stratified fluids, and the particles or organisms larger than this length scale are significantly affected by the stratification [15,23]. As their calculation is only valid at low Pe, we expect to have a different length scale at high Pe. This length scale $L = (\nu u_c / N^2)^{1/3}$ was first noted by Janowitz in the context of horizontally towed two-dimensional (2D) particles in stratified fluids [24] and was recently used by Zhang *et al.* while discussing the mechanism behind the drag enhancement in stratified fluids [25]. As the density transport is dominated by advection at high Pe, it is of no surprise that this length scale depends on the characteristic velocity u_c, which is either the settling velocity of a particle or the self-propulsion velocity of an organism. For weak stratification, as is of interest to us, these stratification length scales are similar to the Oseen length scale $l_o = \nu / u_c$ that exists in the context of small inertia in homogeneous fluids. In the inertial case, inertia is negligible in the near-field and hence the flow due to particle and neutrally buoyant organism decays as $\frac{1}{r}$ and $\frac{1}{r^2}$ at $r \gg a$, respectively, where r is the distance measured from the center of the particle or the organism. On the other hand, in the far field, at $r \approx l_o$, the inertial forces become as important as the viscous forces and the flow decays differently from that in the Stokes flow limit. Similarly for weak stratifications, the buoyancy forces are negligible in the near field while they become as important as the viscous forces in the far field. Our focus is to analyze the flow in this far field. As expected, the size of the particle or the organism is unimportant in the far field, so the relevant length scale is the stratification length.

We organize this paper as follows: We derive the far-field flow due to a towed particle and a swimming organism in a stratified fluid at both low and high Pe and analyze the flow at high Pe in Sec. II. Using these flow fields, we then derive and analyze the drift induced by a towed drop and a swimming organism in a stratified fluid at both low and high Pe in Sec. III and provide a few concluding remarks in Sec. IV. We always assume that the swimming organism is neutrally buoyant.

II. FLOW FAR AWAY FROM A PARTICLE OR AN ORGANISM IN A DENSITY-STRATIFIED FLUID

Consider a particle or a drop towed with velocity $\mathbf{u} = u_3 \mathbf{e}_3$ or a neutrally buoyant swimming organism with the self-propulsion velocity of $\mathbf{u} = u_3 \mathbf{e}_3$ in a linearly density-stratified fluid. The ambient density of the stratified fluid decreases linearly with an increase in height as $\rho_0 = \rho_\infty - \gamma x_3$. Here,

ρ_∞ is the reference density, $\gamma > 0$ is the ambient density gradient, $\mathbf{x} = x_j \mathbf{e}_j$ is the position vector in the laboratory frame of reference, $\mathbf{e}_j$ are the unit vectors along the coordinate axes in the Cartesian coordinate system, and $\mathbf{e}_3$ points vertically upwards. Neutrally buoyant means the hydrostatic force acting on the particle or organism balances the weight. The hydrostatic force or buoyancy can be found by considering a stationary particle in a stratified fluid and it turns out to be the weight of the ambient fluid displaced. Hence, a particle or organism is neutrally buoyant in a linearly stratified fluid if its density is equal to the ambient fluid density evaluated at its center.

In a comoving frame, the flow is governed by the continuity and the Navier-Stokes equations, which under the Boussinesq approximation [26,27] are given as

$$\nabla \cdot \mathbf{w} = 0, \tag{1}$$

$$\rho_\infty \left(\frac{\partial \mathbf{w}}{\partial t} + \mathbf{w} \cdot \nabla \mathbf{w} \right) = -\nabla p + \rho_\infty \nu \nabla^2 \mathbf{w} - \rho g \mathbf{e}_3 - \rho_\infty \frac{d\mathbf{u}}{dt}. \tag{2}$$

Usually, the stratification in the temperature or the salt concentration leads to the density stratification and, for small changes in the former, the change in the density is linearly related to the change in the temperature or the salt concentration and we can directly write an advection-diffusion equation for density instead of such an equation for temperature or salt concentration:

$$\frac{\partial \rho}{\partial t} + \mathbf{w} \cdot \nabla \rho = \kappa \nabla^2 \rho. \tag{3}$$

Far away from the particle or the organism, the fluid velocity approaches the negative of the towed or the self-propulsion velocity while the density approaches the ambient density:

$$\text{as } r \to \infty, \quad \mathbf{w} \to -\mathbf{u}, \quad \rho \to \rho_0 = \rho_\infty - \gamma x_3. \tag{4}$$

Here, $\mathbf{r} = r_j \mathbf{e}_j$ is a position vector in the comoving frame with the origin located at the center of the particle or the organism and $r = |\mathbf{r}|$. The position vectors in the laboratory and the comoving frame are related by $\mathbf{x} = \mathbf{r} + \mathbf{x}_s$, where $\mathbf{x}_s$ locates the center of the particle or the organism. On the surface of the particle or the organism, we apply a no-flux boundary condition for the density which holds if the surface is impermeable to the concentration or insulating to the temperature field:

$$\text{On the surface: } \mathbf{n} \cdot \nabla \rho = 0. \tag{5}$$

On the surface, we also have the usual kinematic and the no-slip boundary conditions for the flow field.

Now, we express all the variables in terms of the disturbance variables denoted by primes as follows:

$$\mathbf{w} = \mathbf{w}' - \mathbf{u}, \quad \rho = \rho' + \rho_0, \quad p = p' + p_0, \tag{6}$$

where p_0 satisfies the equation $-\nabla p_0 - \rho_0 g \mathbf{e}_3 = \mathbf{0}$. Assuming the quasisteady conditions to hold, the governing equations

written in terms of the disturbance variables are given by

$$\nabla \cdot \mathbf{w}' = 0, \tag{7}$$

$$\rho_\infty(\mathbf{w}' \cdot \nabla \mathbf{w}' - \mathbf{u} \cdot \nabla \mathbf{w}') = -\nabla p' + \rho_\infty \nu \nabla^2 \mathbf{w}' - \rho' g \mathbf{e}_3, \tag{8}$$

$$\mathbf{w}' \cdot \nabla \rho' - \mathbf{u} \cdot \nabla \rho' - \mathbf{w}' \cdot \mathbf{e}_3 = \kappa \nabla^2 \rho'. \tag{9}$$

By definition, all the disturbance variables decay to zero far away from the particle or the organism

$$\mathbf{w}' = \mathbf{0}, \quad \rho' = 0 \quad \text{as} \quad r \to \infty. \tag{10}$$

We use the characteristic velocity scale u_c, which is either u_3 or $6\pi u_3$, the characteristic length scale a quantifying the size of the particle or the organism, the viscous pressure scale $p_c = \frac{\rho_\infty \nu u_c}{a}$, and the density scale $\rho_c = \gamma a$ to nondimensionalize the velocity, length, pressure, and density, respectively. If u_c is u_3 (resp. $6\pi u_3$), then the dimensionless u_3 is 1 (resp. $1/6\pi$). The dimensionless governing equations are then given as follows:

$$\nabla \cdot \mathbf{w}' = 0, \tag{11}$$

$$\text{Re}(\mathbf{w}' \cdot \nabla \mathbf{w}' - \mathbf{u} \cdot \nabla \mathbf{w}') = -\nabla p' + \nabla^2 \mathbf{w}' - \text{Ri}\rho' \mathbf{e}_3, \tag{12}$$

$$\text{Pe}(\mathbf{w}' \cdot \nabla \rho' - \mathbf{u} \cdot \nabla \rho' - \mathbf{w}' \cdot \mathbf{e}_3) = \nabla^2 \rho'. \tag{13}$$

Here, Re, Pe, Ri are, respectively, the Reynolds, the Péclet, and the viscous Richardson numbers, which are the ratio of the inertia to the viscous forces, the advective to the diffusive transport rate of density, and the buoyancy to the viscous forces [28]. Their precise expressions are given by

$$\text{Re} = \frac{a u_c}{\nu}, \quad \text{Pe} = \frac{a u_c}{\kappa}, \quad \text{Ri} = \frac{\gamma g a^3}{\rho_\infty \nu u_c}. \tag{14}$$

For small Re, Ri, the disturbance flow far away from a particle or an organism decays at least as fast as $1/r$. More precisely, for $1 \ll r < \min\{\frac{l}{a}, \frac{L}{a}, \frac{l_o}{a}\}$, $\mathbf{w}' \sim \frac{1}{r}, \frac{1}{r^2}$ for the towed particle and the neutrally buoyant swimming organism, respectively. The towed velocity of the particle $\mathbf{u}$ is constant. The self-propulsion velocity of an organism, although is affected by stratification, can be taken as a constant, equal to this velocity in a homogeneous fluid as far as the calculation of the leading-order disturbance variables far away from the organism are concerned. So, in the far field $r \gg 1$, $\mathbf{w}' \ll \mathbf{u}$ and hence $\mathbf{w}' \cdot \nabla \mathbf{w}' \ll \mathbf{u} \cdot \nabla \mathbf{w}'$ and $\mathbf{w}' \cdot \nabla \rho' \ll \mathbf{u} \cdot \nabla \rho'$. As a towed particle exerts a force $F\mathbf{e}_3$ on the fluid while a neutrally buoyant organism exerts a symmetric force-dipole or stresslet $-b\mathbf{e}_3\mathbf{e}_3$ on the fluid, they appear as a point force and a symmetric force-dipole, respectively, in the far field. Again, the stratification affects the force and the stresslet exerted but these can be taken as their values in the homogeneous fluid for the purpose of finding the leading-order disturbance variables. In homogeneous fluids, F should be linearly related to u_3, i.e., $F = Ku_3$. This description of the particle holds only if it is nonskew and is settling along one of its principal axes for translation [29]. Otherwise, a simple unidirectional settling can lead to a force in all three directions. Examples of nonskew shapes are sphere, spheroid, ellipsoid, disk, weakly deformed sphere, etc. For a sphere, $K = 6\pi$ and, for a drop, $K = 2\pi\mathcal{R}$, $\mathcal{R} = (3\lambda + 2)/(\lambda + 1)$, where λ is the viscosity ratio of the inner fluid to the outer fluid. Also, the stresslet

strength $b > 0$ for pusher-type organisms that push the fluid behind them to propel while $b < 0$ for puller-type organisms which pull the fluid in front of them to swim. Examples of pusher- and puller-type organisms are *Escherichia coli* and *Chlamydomonas*, respectively. Hence, in the far field, we neglect the terms $\mathbf{w}' \cdot \nabla \mathbf{w}'$, $\mathbf{w}' \cdot \nabla \rho'$ in Eqs. (12) and (13), and replace the boundary conditions on the surface of the particle and the organism, respectively with the source terms $F\mathbf{e}_3\delta(\mathbf{r})$ and $-b\mathbf{e}_3\mathbf{e}_3 \cdot \nabla\delta(\mathbf{r})$ in the Navier-Stokes equations. The no-flux boundary condition for the density on the particle or organism's surface prohibits the occurrence of such source terms in the advection-diffusion equation. Hence, in the far-field, the equations governing the disturbance variables are given as

$$\nabla \cdot \mathbf{w}' = 0, \tag{15}$$

$$-\text{Re}\,\mathbf{u} \cdot \nabla \mathbf{w}' = -\nabla p' + \nabla^2 \mathbf{w}' - \text{Ri}\rho' \mathbf{e}_3$$
$$+ \left\{ \begin{array}{c} F\mathbf{e}_3\delta(\mathbf{r}) \\ -b\mathbf{e}_3\mathbf{e}_3 \cdot \nabla\delta(\mathbf{r}) \end{array} \right\}, \tag{16}$$

$$-\text{Pe}(\mathbf{u} \cdot \nabla \rho' + \mathbf{w}' \cdot \mathbf{e}_3) = \nabla^2 \rho'. \tag{17}$$

Note that F and b, respectively, are nondimensionalized by $\rho_\infty \nu a u_c$ and $\rho_\infty \nu a^2 u_c$. These equations are coupled yet linear. Hence, we have

Far-field flow due to an organism

$$= -\frac{b}{F}(\mathbf{e}_3 \cdot \nabla) \quad \text{(Far-field flow due to a towed particle)}, \tag{18}$$

a relationship that holds for homogeneous fluids [30], now is also true for stratified fluids. Given this relationship, we only focus on deriving the flow due to a towed particle and we neglect inertia for simplicity. Using a different formalism, these equations governing the far-field disturbance variables were already derived earlier for a towed spherical particle [20,31–33] but here we generalize such a derivation to neutrally buoyant swimming organisms.

At low Pe, far from the particle, the characteristic length scale should be the relevant stratification length scale l instead of the particle size a. Hence, we nondimensionalize the length by l or, equivalently, rescale the dimensionless length as $\bar{r} = \epsilon r$, where $\epsilon = a/l = (\text{RiPe})^{1/4}$. This limit of small Ri, Pe means that ϵ is small. Far away from the particle, at $r \sim \frac{l}{a} = \frac{1}{\epsilon} \gg 1$, the velocity and the pressure disturbance decay as $\mathbf{w}' \sim \frac{1}{r} \sim \epsilon$, $p' \sim \frac{1}{r^2} \sim \epsilon^2$, so we rescale these variables as $\mathbf{w}' = \epsilon\bar{\mathbf{w}}'$, $p' = \epsilon^2\bar{p}'$ so that the rescaled variables are $O(1)$. Also, far away from the particle, at $r \sim \frac{1}{\epsilon}$, the viscous terms $\nabla^2\mathbf{w}'$ are $O(\epsilon^3)$. To make it explicit that the buoyancy terms $\text{Ri}\rho'$ are of the same order of magnitude as the viscous terms and also to have an $O(1)$ density field, we rescale the density as $\rho' = \frac{\text{Pe}}{\epsilon}\bar{\rho}'$. Hence, the equations governing the rescaled variables at low Pe, Pe $\ll \epsilon$, are given by

$$\bar{\nabla} \cdot \bar{\mathbf{w}}' = 0, \tag{19}$$

$$\mathbf{0} = -\bar{\nabla}\bar{p}' + \bar{\nabla}^2\bar{\mathbf{w}}' - \bar{\rho}'\mathbf{e}_3 + F\mathbf{e}_3\delta(\bar{\mathbf{r}}), \tag{20}$$

$$-\bar{\mathbf{w}}' \cdot \mathbf{e}_3 = \bar{\nabla}^2\bar{\rho}'. \tag{21}$$

These equations governing the far-field disturbance caused by a towed particle are the same as those governing the disturbance due to a point-force placed in a stratified fluid at low Re, Pe which were derived by Ardekani and Stocker [15]. Because these equations are linear, we solve them in Fourier space, where the definition of the Fourier and the inverse Fourier transforms are given as

$$\hat{\bar{\mathbf{w}}}'(\mathbf{k}) = \int \bar{\mathbf{w}}'(\bar{\mathbf{r}})e^{-i\mathbf{k}\cdot\bar{\mathbf{r}}}d\bar{\mathbf{r}}, \quad \bar{\mathbf{w}}'(\bar{\mathbf{r}}) = \frac{1}{8\pi^3}\int \hat{\bar{\mathbf{w}}}'(\mathbf{k})e^{i\mathbf{k}\cdot\bar{\mathbf{r}}}d\mathbf{k}. \tag{22}$$

Here, $\hat{\bar{\mathbf{w}}}'(\mathbf{k})$ is the Fourier transform of $\bar{\mathbf{w}}'$, $i = \sqrt{-1}$, and $\mathbf{k} = k_j\mathbf{e}_j$. The far-field disturbance flow caused by a towed particle in the Fourier space is given by [17,20,31,32]

$$\hat{\bar{\mathbf{w}}}'(\mathbf{k}) = \frac{Fk^2}{k^6 + k^2 - k_3^2}\big[-k_1k_3\mathbf{e}_1 - k_2k_3\mathbf{e}_2 + (k^2 - k_3^2)\mathbf{e}_3\big], \tag{23}$$

where $k = \sqrt{\mathbf{k}\cdot\mathbf{k}}$.

For a swimming organism, the far-field flow decays as $\mathbf{w}' \sim \frac{1}{r^2} \sim \epsilon^2$ at $r \sim \frac{1}{\epsilon}$, so we should rescale the flow as $\mathbf{w}' = \epsilon^2\bar{\mathbf{w}}'$. Because of Eq. (18), the far-field flow due to an organism in Fourier space is simply $-\frac{b}{F}ik_3$ times the far-field flow due to a towed particle in the Fourier space. Hence, we have the following expression for the flow far away from an organism in the Fourier space

$$\hat{\bar{\mathbf{w}}}'(\mathbf{k}) = \frac{ibk_3k^2}{k^6 + k^2 - k_3^2}\big[k_1k_3\mathbf{e}_1 + k_2k_3\mathbf{e}_2 - (k^2 - k_3^2)\mathbf{e}_3\big]. \tag{24}$$

At high Pe, the characteristic length scale in the far-field should be the appropriate stratification length scale L. Hence, we use L to nondimensionalize length or rescale the dimensionless length as $\bar{r} = \mathrm{Ri}^{1/3}r$, where $\mathrm{Ri}^{1/3}$ can be interpreted as the ratio a/L. In the far-field of the particle, at $r \sim \frac{L}{a} = \frac{1}{\mathrm{Ri}^{1/3}} \gg 1$, the flow and the pressure disturbance decay as $\mathbf{w}' \sim \frac{1}{r} \sim \mathrm{Ri}^{1/3}$, $p' \sim \frac{1}{r^2} \sim \mathrm{Ri}^{2/3}$, hence we rescale these variables as $\mathbf{w}' = \mathrm{Ri}^{1/3}\bar{\mathbf{w}}'$, $p' = \mathrm{Ri}^{2/3}\bar{p}'$ so as to have $O(1)$ rescaled variables. Also, in the far-field of the particle, at $r \sim \frac{1}{\mathrm{Ri}^{1/3}}$, the viscous terms $\nabla^2\mathbf{w}'$ are $O(\mathrm{Ri})$. These viscous terms are in balance with the buoyancy terms $\mathrm{Ri}\rho'$ provided that the density disturbance ρ' is $O(1)$. Since ρ' is $O(1)$, it does not need to be rescaled. Hence, the equations governing the rescaled variables at high Pe, Pe $\gg \mathrm{Ri}^{1/3}$, are given by

$$\bar{\nabla}\cdot\bar{\mathbf{w}}' = 0, \tag{25}$$

$$\mathbf{0} = -\bar{\nabla}\bar{p}' + \bar{\nabla}^2\bar{\mathbf{w}}' - \rho'\mathbf{e}_3 + F\mathbf{e}_3\delta(\bar{\mathbf{r}}), \tag{26}$$

$$-\mathbf{u}\cdot\bar{\nabla}\rho' - \bar{\mathbf{w}}'\cdot\mathbf{e}_3 = 0. \tag{27}$$

We solve these equations in Fourier space to find the following expression for the Fourier transform of the disturbance flow [17,20,31,32]:

$$\hat{\bar{\mathbf{w}}}' = \frac{Fu_3k_3}{k^4u_3k_3 + i(k^2 - k_3^2)}\big[-k_1k_3\mathbf{e}_1 - k_2k_3\mathbf{e}_2 + (k^2 - k_3^2)\mathbf{e}_3\big]. \tag{28}$$

As the flow far from an organism $r \sim \frac{1}{\mathrm{Ri}^{1/3}}$ decays as $\mathbf{w}' \sim \frac{1}{r^2} \sim \mathrm{Ri}^{2/3}$, we rescale this flow as $\mathbf{w}' = \mathrm{Ri}^{2/3}\bar{\mathbf{w}}'$. Similar to low-Pe analysis, in the Fourier space, the far-field flow due to an organism is given by $-\frac{b}{F}ik_3$ times the far-field flow

due to a towed particle, and hence we have the following expression for the former flow field:

$$\hat{\bar{\mathbf{w}}}' = \frac{ibu_3k_3^2}{k^4u_3k_3 + i(k^2 - k_3^2)}\big[k_1k_3\mathbf{e}_1 + k_2k_3\mathbf{e}_2 - (k^2 - k_3^2)\mathbf{e}_3\big]. \tag{29}$$

As the far-field flow at low Pe was already analyzed by Ardekani and Stocker [15], we focus our attention on analyzing the far-field flow at high Pe. We plot this far-field flow due to a towed spherical particle and a pusher-type organism in Figs. 1 and 2, respectively, where the former and the latter flows are found by performing an inverse Fourier transform of Eqs. (28) and (29) using the ifft function in MATLAB [34]. In these figures, we also compare the spatial decay of the vertical velocity at high Pe with that at low Pe as well as that in homogeneous fluids. We choose $u_c = 6\pi u_3$ to have unit point force in Fig. 1 while we choose $u_c = u_3$, $b = 1$ in Fig. 2.

It is clear that the flow at high Pe is fore-aft asymmetric. The presence of the $\mathbf{u}\cdot\bar{\nabla}\rho'$ term in the advection-diffusion equation that transports the density in only one direction (vertically upwards in our case) leads to such fore-aft asymmetry. This advective term $\mathbf{u}\cdot\bar{\nabla}\rho'$ is absent at low Pe, due to which the far-field flow due to a towed particle and organism is, respectively, fore-aft symmetric and fore-aft mirror symmetric similar to the counterparts in the homogeneous fluid. Fore-aft asymmetry resulting from the presence of an advective term of the form $\mathbf{u}\cdot\bar{\nabla}\rho'$ can also be observed in a simpler situation of the forced convective heat transfer from a sphere placed in a uniform streaming flow at low Re, high Pe (see Chapter 9 in Ref. [26]). This fore-aft asymmetry at high Pe means that the spatial decay in the upstream ($\bar{r}_3 > 0$) is different from the decay in the downstream ($\bar{r}_3 < 0$). Compare the red solid line with the red dash-dotted line in Figs. 1(b) and 2(b).

In stratified fluids, the buoyancy of the entrained fluid as well as the tendency of the perturbed isopycnals to return to their neutrally buoyant position together contribute to suppressing the vertical motion. This nature of stratification has two consequences on the flow induced by a towed particle or a swimming organism. First, the flow in the stratified fluid at both low and high Pe decays faster than that in the homogeneous fluid [see Figs. 1(b) and 2(b)]. Second, the streamlines in the stratified fluid are closed, unlike the open streamlines in a homogeneous fluid. These consequences of stratification on the flow field can also be understood by imagining the stratification to act as horizontal virtual walls since walls also suppress the vertical motion. Then it is of no surprise that the far-field flow due to a towed particle in a stratified fluid is qualitatively similar to the flow due to a point-force located in between two horizontal walls in a homogeneous fluid. The fore-aft symmetry (resp. asymmetry) of the flow at low Pe (resp. high Pe) means that the equivalent situation in a homogeneous fluid consists of a point-force located symmetrically (resp. asymmetrically) between two walls. Compare Fig. 1(c) with the flow in Fig. 1(a) in the region $-0.5 < \bar{r}_3 < 1$.

At high Pe, the flow due to a towed particle in the upstream decays slower than the flow in the downstream, but this flow in both the upstream and the downstream decays faster than the flow at low Pe [see Fig. 1(b)]. Because the flow due to an organism is proportional to the vertical derivative of the flow due to a towed particle [see Eq. (18)], the slow decay
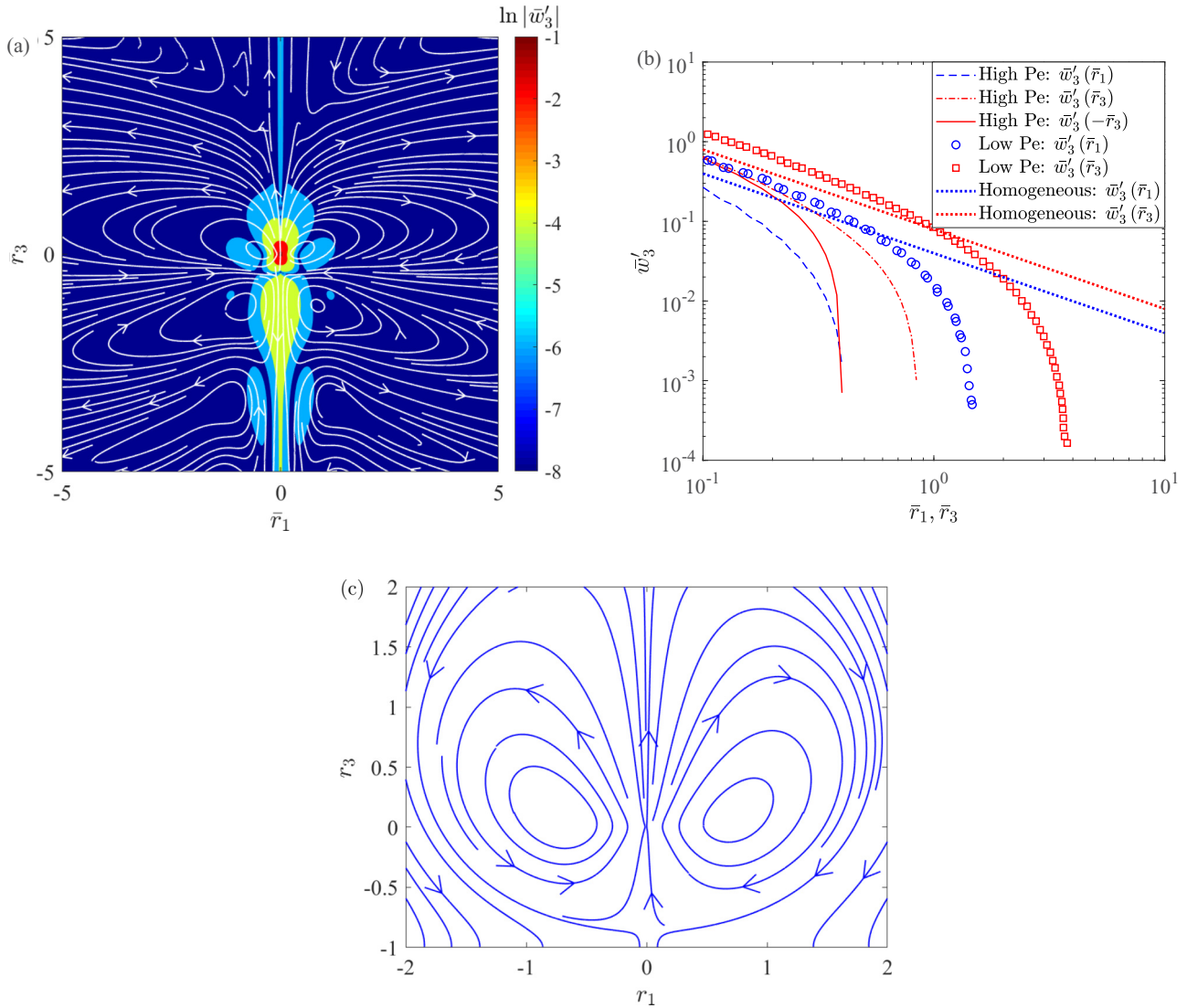
FIG. 1. Flow due to a towed sphere in the far field or that due to a point-force. The sphere is towed and the point-force is oriented in the vertically upward direction. (a) Filled contours of $\ln |\bar{w}_3'|$ along with the streamlines in a stratified fluid at high Pe. (b) The spatial variation of the vertical velocity along horizontal (blue) and vertical (red) directions. The data in the homogeneous fluids are shown by dotted lines whereas those in stratified fluids at low Pe are shown by symbols and those at high Pe are shown by dashed, solid, and dash-dotted lines. At high Pe, dash-dotted and solid lines show the vertical variation along the upstream and the downstream directions, respectively. The data at low Pe is taken from Fig. 2(a) of Ref. [15]. (c) Streamlines associated with the flow caused by a point-force located asymmetrically between two horizontal walls in a homogeneous fluid. One wall is at $r_3 = -1$ while the other is at $r_3 = 8$. This flow is found by adding the image flow due to the walls [35,36] to the Stokeslet flow. Such a simple calculation yields inaccurate flow far from the point-force, which justifies the nonzero velocities seen near the bottom wall.

of the flow due to a towed particle in the upstream explains the similar slow decay of the flow due to an organism in the upstream compared with the flow decay in the downstream at high Pe [see Fig. 2(b)]. Unlike the flow due to a towed particle, the flow due to an organism in the upstream at high Pe decays slower than that at low Pe whereas, in the downstream, the flow at high Pe decays faster than that at low Pe [see Fig. 2(b)].

III. DRIFT

An initially marked (as in with a dye) plane of fluid deforms due to the motion of the particle or the organism normal to this marked fluid plane. The volume enclosed between the initial and final profiles of marked fluid is termed the partial drift volume D_p [37,38]. When the extent of the marked fluid as well as the distance traveled by the particle or the organism relative to the marked fluid are infinite, the enclosed volume is referred to as the drift volume. See Fig. 3 for a schematic of the partial drift volume. In the context of towed particles or drops, we analyze both the partial drift and the drift volume. But since most of the organisms travel in a straight line only for finite time periods before reorienting due to thermal or biological noise, we only focus on discussing partial drift induced by the organisms.

In line with the previous works [17,30,38], we choose $u_c = u_3$ and assume the particle is towed or the organism is
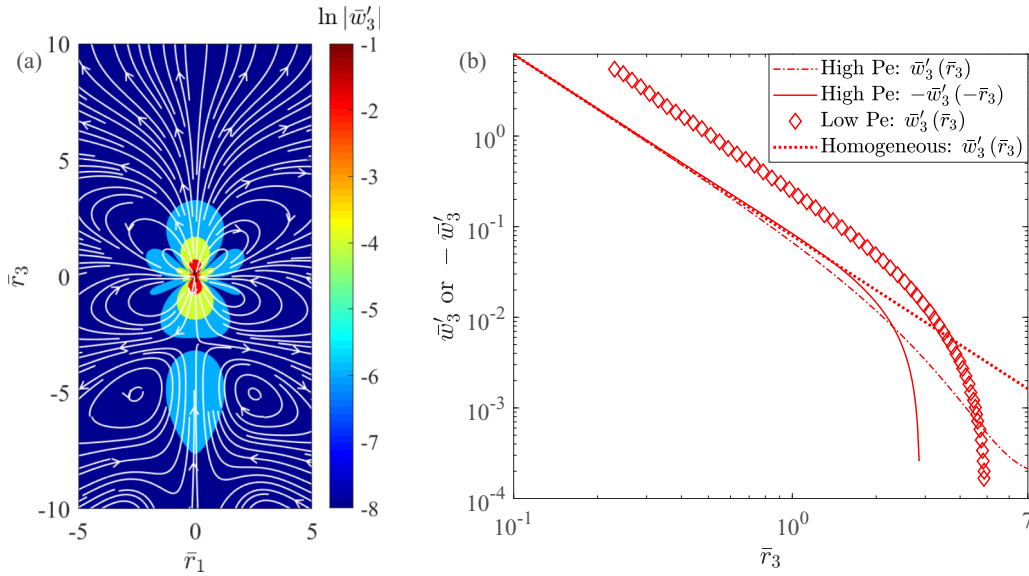
FIG. 2. Far-field flow due to a vertically oriented ($u_3 > 0$) pusher swimmer ($b = 1$). (a) Filled contours of $\ln |\bar{w}'_3|$ along with the streamlines in a stratified fluid at high Pe. (b) The vertical variation of the vertical velocity. The line style and color follow the same notation as that given in Fig. 1(b). The data at low Pe are taken from Fig. 2(a) of Ref. [15].

oriented in the vertically upward direction, i.e., $u_3 > 0$. Also, we consider the initially marked plane of fluid to be disk shaped with finite radius and zero thickness. We choose the center of the marked fluid disk as the origin of the coordinate axes in the laboratory frame. Recall that the origin in the comoving frame is at the center of the particle or the organism. We denote the axial and radial coordinates associated with the
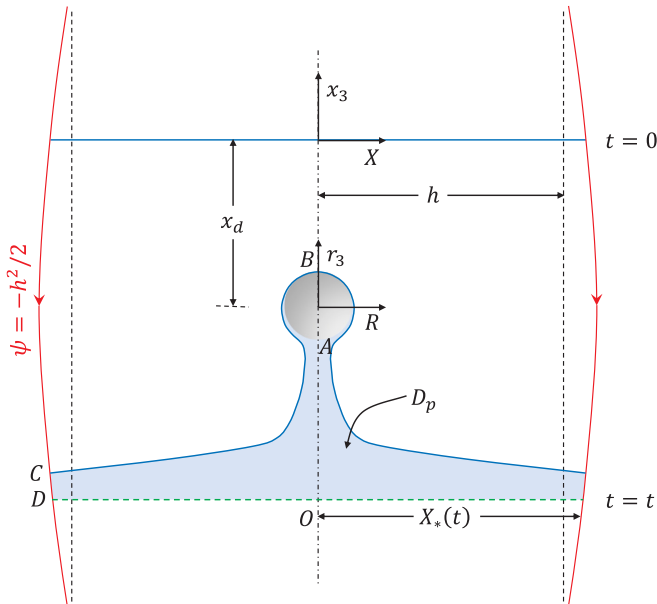

FIG. 3. Schematic showing the definition of the partial drift volume D_p. In the comoving frame, the drop or organism is stationary and the marked fluid is initially at a distance x_d upstream of the drop or swimmer. At time t, the marked fluid deforms as it passes the drop or swimmer. The volume enclosed between the deformed (blue curve) and the undeformed (green line) marked fluids at time t determines the partial drift at that time (light blue region).

cylindrical coordinate system in the laboratory frame by x_3, X while those in the comoving frame by r_3, R. At time $t = 0$, the particle or the organism has not yet crossed the marked fluid and the separation between them is denoted by x_d, i.e., $\mathbf{x}_s \cdot \mathbf{e}_3|_{t=0} = -x_d$. Hence $\mathbf{x}_s \cdot \mathbf{e}_3 = -x_d + t$, which means that $r_3 = x_3 - \mathbf{x}_s \cdot \mathbf{e}_3 = x_3 + x_d - t$ and also $R = X$. The flow in the laboratory frame is the same as the disturbance flow in the comoving frame. We denote the stream function associated with the flow in the laboratory and comoving frame by ψ', ψ, respectively. As the flow in these two frames differ by a unit uniform streaming velocity, the corresponding stream functions should differ by $X^2/2$, i.e., $\psi' = \psi + \frac{X^2}{2}$. In the comoving frame, far away from the particle or the organism, the flow approaches the negative of the towed or the self-propulsion velocity, hence $\psi \to -\frac{X^2}{2}$ and one such streamline $\psi = -\frac{h^2}{2}$ intersects the edge of the marked fluid and also defines the extent of the marked fluid. In the laboratory frame, we denote this intersection point and the stream function at this point by $(x_3, X) = (0, X_*(t))$, $\psi'_*(t)$, respectively.

In the laboratory frame, we apply conservation of mass to the control volume $OABCD$, use the Boussinesq approximation, and express the velocity in terms of the stream function to derive the following expression for the partial drift:

$$D_p = 2\pi \int_0^t \psi'_*(t')dt' - [V_b(t) - V_b(0)]. \qquad (30)$$

See Ref. [17] for more details of this derivation. Here $V_b(t)$ denotes the volume of the particle or the organism that crossed the marked fluid $x_3 = 0$ by time t. Because of the Boussinesq approximation, this expression for the partial drift in the stratified fluids is the same as that in the homogeneous fluids [30,38].

We do the calculation for the large marked fluid radius as compared with the size of the drop or the organism, i.e., $h \gg 1$. In this limit, to find the leading-order drift, we use

the following three arguments to simplify the above equation for D_p. First, since the extent of the marked fluid is large, the streamlines at the edge of the marked fluid should approach the free stream position and hence we neglect the deflection of streamlines at the edge of the marked fluid relative to the free stream position. This means that $X_* = h$ and $\psi'_*(t) = \psi'(x_3 = 0, X = h, t) = \psi'(r_3 = x_d - t, R = h, t)$. Defining $\tau = \frac{t - x_d}{h}$ and $\tau_0 = -\frac{x_d}{h}$, we get

$$D_p = 2\pi h \int_{\tau_0}^{\tau} \psi'_*(\tau')d\tau' - [V_b(\tau) - V_b(\tau_0)]. \quad (31)$$

Second, since we are interested in scenarios where the drift is large compared with the volume of the particle or the organism, we neglect the term in the brackets because it is of the order of the particle volume i.e., $O(1)$, and hence much smaller than the drift. This argument can be verified *a posteriori*. Third, a large extent of the marked fluid means that the stream function at the edge of the marked fluid ψ'_* depends only on the flow field far away from the particle or the organism that is governed by Eqs. (15)–(17). If the partial drift or the drift, $D_p(\tau_0 \to -\infty, \tau \to \infty)$, turns out to be zero from this leading-order calculation, we need to consider the effect of these neglected contributions to find the higher-order drift, but such a calculation is beyond the scope of the present paper.

A. Drift due to a towed drop

The rescalings at low- or high-Pe mentioned in the previous section mean that the far-field stream function should be rescaled as $\psi' = \bar{\psi}'/\xi$, where $\xi = \epsilon$, $\mathrm{Ri}^{1/3}$ at low and high Pe, respectively. In the Fourier space, since the far-field flow is readily known, Eqs. (23) and (28), we can find the far-field stream function $\hat{\bar{\psi}}'$ from this velocity field using (see the Appendix)

$$\hat{\bar{\psi}}' = -\frac{1}{k_3}\left(\frac{\partial \hat{\bar{w}}'_1}{\partial k_1} + \frac{\partial \hat{\bar{w}}'_2}{\partial k_2}\right). \quad (32)$$

Expressing ψ' in Eq. (31) in terms of $\hat{\bar{\psi}}'$ through the inverse Fourier transform and simplifying the resulting integral yields the following expression for D_p:

$$D_p = -\frac{ih^2}{2\pi\xi_h^2}\int_{-\infty}^{\infty} dk_3 \int_0^{\infty} dk_r \hat{\bar{\psi}}'(k_r, k_3)k_r J_0(\xi_h k_r)$$
$$\times \frac{(e^{-i\xi_h k_3 \tau_0} - e^{-i\xi_h k_3 \tau})}{k_3}. \quad (33)$$

See Ref. [17] for details of this simplification. Here, $k_r = (k_1^2 + k_2^2)^{1/2}$, J_0 is the Bessel function of the first kind and zeroth order while $\xi_h = \xi h = \frac{h}{l}, \frac{h}{L}$, respectively, at low and high Pe. So ξ_h is the ratio of the marked fluid radius to the stratification length scale and a high value of ξ_h means that a major portion of the marked fluid and hence the drift are significantly affected by the stratification. We denote ξ_h at low and high Pe by $\epsilon_h = \epsilon h = h/l$ and $\mathrm{Ri}_h^{1/3} = \mathrm{Ri}^{1/3}h = h/L$, respectively.

At both low and high Pe, we can find D_p by using this equation and the following expressions for $\hat{\bar{\psi}}'$:

$$\frac{\hat{\bar{\psi}}'}{F} = \begin{cases} \dfrac{2\left(k_3^8 + 2k_3^6 k_r^2 - 2k_3^2 k_r^6 - k_r^8 + k_r^4\right)}{\left(k_3^6 + 3k_3^4 k_r^2 + 3k_3^2 k_r^4 + k_r^6 + k_r^2\right)^2} & \text{at low Pe} \\[4mm] \dfrac{2u_3^2 k_3^2\left(k_3^4 - k_r^4\right)}{\left(k_3^5 u_3 + 2u_3 k_3^3 k_r^2 + u_3 k_3 k_r^4 + ik_r^2\right)^2} & \text{at high Pe,} \end{cases} \quad (34)$$

where $F = 2\pi \mathcal{R} u_3$ for a drop and $u_3 = 1$. At low Pe, we already did this calculation and reported the drift induced by a towed drop in our recent paper [17]. Using $\tau_0 = -10$, we plot the variation of D_p with τ, ϵ_h, or $\mathrm{Ri}_h^{1/3}$ at low and high Pe in Fig. 4. From this figure, we see that the drift in stratified fluids is less than that in homogeneous fluids. In stratified fluids, with an increase in the stratification as exemplified by an increase in ϵ_h or $\mathrm{Ri}_h^{1/3}$ for fixed h, the partial drift decreases. These two observations are a manifestation of the stratification's effect in suppressing the vertical flow. This is because this effect of stratification leads to closed streamlines and also causes the flow to decay rapidly with position, both of which reduce the drift.

At low Pe, the fore-aft flow symmetry means that the upstream drift is equal to the downstream drift, i.e., $-D_p(\tau = -\tau_c, \tau_0 = 0, h) = D_p(\tau = \tau_c, \tau_0 = 0, h)$ for any $\tau_c > 0$. Here, the upstream (downstream) drift is the drift induced before (after) the drop has crossed the marked fluid. A lack of such symmetry at high Pe means that the upstream drift is definitely not equal to the downstream drift. But a slower decay of velocity field in the upstream than that in the downstream [see Fig. 1(b)] and a sizable reverse flow in the downstream [see Fig. 1(a) for $\bar{r}_3 < -0.5$ and $|\bar{r}_1| < 1$] makes the upstream drift larger than the downstream drift at high Pe.

It is interesting to compare the drift induced by a towed particle or drop in a stratified fluid at high Pe with that induced in a homogeneous fluid at small or finite Re. In the latter case, the flow is again fore-aft asymmetric but now, due to $\mathbf{u} \cdot \nabla \mathbf{w}'$, this leads to unequal upstream and downstream drifts. At a non-zero Re in a homogeneous fluid, because the flow in the downstream wake decays slower than that in the upstream, the downstream drift is larger than the upstream drift.

In homogeneous fluids, the slow decay of velocity with position as well as the open streamline flow lead to the divergence of the partial drift with time as $\tau_0 \to -\infty$ or $\tau \to \infty$. Hence, small particles or drops towed in homogeneous fluids can drag an infinite volume of fluid with them. Far away from the towed particle or drop, at $r \sim \frac{l}{a}$ or $\frac{L}{a}$, the stratification cuts off this slow decay and closes the streamlines, and this effect of stratification eliminates the divergence of D_p as $\tau_0 \to -\infty$ or $\tau \to \infty$. For instance, this is demonstrated in Fig. 4 at $2\epsilon_h = 2\mathrm{Ri}_h^{1/3} = 1$ where D_p asymptotes to a constant value as $-\tau_0$, τ approach 10 or more. Hence, the drift, an asymptotic value of D_p in the limit $\tau_0 \to -\infty$ and $\tau \to \infty$ in the stratified fluids is finite. At low Pe, the drift is nonzero, as demonstrated again by the curve at $2\epsilon_h = 1$ in Fig. 4(a). This drift found from the leading-order calculation is $O(h^2)$ [see Eq. (33)] and as $h \gg 1$, a towed drop in the stratified fluid at low Pe drags a large volume of fluid relative to its own volume. At high Pe, the leading-order drift turns out to be zero, as illustrated again
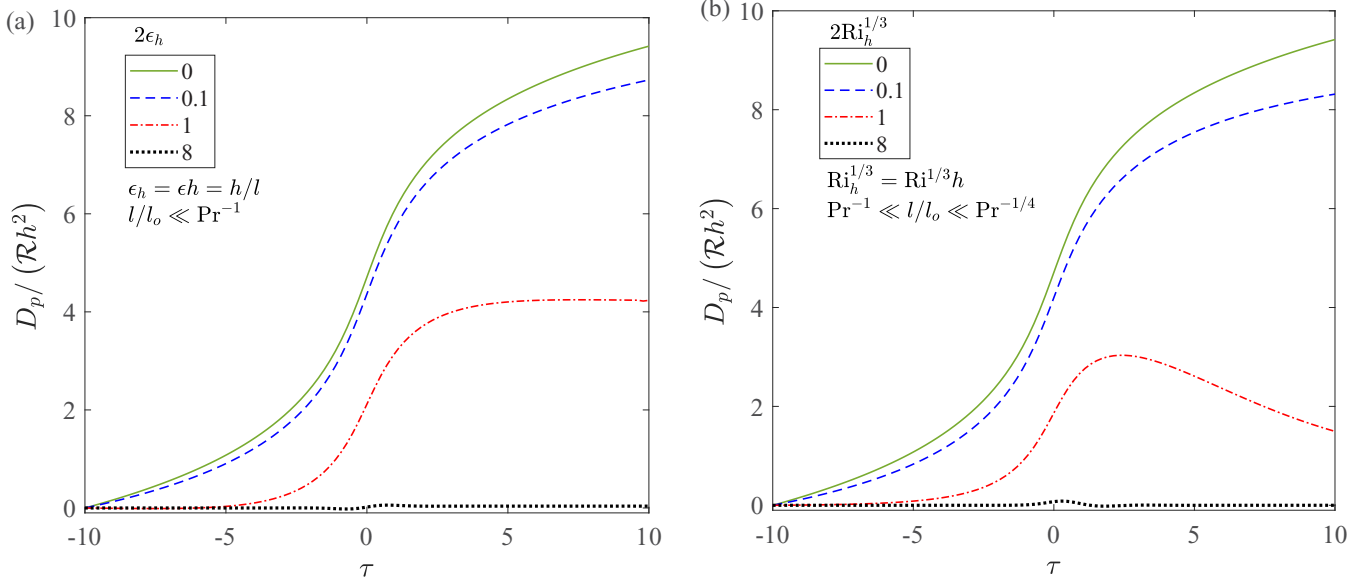
FIG. 4. The variation of the normalized partial drift induced by a towed drop $D_p/\mathcal{R}h^2$ with (a) τ, ϵ_h at low Pe and (b) $Ri_h^{1/3}$ at high Pe. To obtain general results that do not depend on $\mathcal{R}$, h, we normalized D_p by $\mathcal{R}h^2$. Here, we choose $\tau_0 = -10$. The low Pe limit Pe $\ll \epsilon$ is the same as $l/l_o \ll$ Pr^{-1} while the high-Pe and low-Re limit Pe $\gg$ Ri$^{1/3}$, Re $\ll$ Ri$^{1/3}$ is same as Pr$^{-1} \ll l/l_o \ll$ Pr$^{-1/4}$, where Pr $= \nu/\kappa$ is the Prandtl number. Panel (a) is adapted from Ref. [17] with permission from the American Physical Society.

by the curve at $2Ri_h^{1/3} = 1$ in Fig. 4(b) with $\tau_0 = -10$ and $\tau \approx 20$. This zero drift is due to the faster decay of velocity at high Pe than that at low Pe and also due to the sizable reverse flow seen downstream at high Pe. Even though such reverse flow downstream exists at low Pe, it is not as significant as that at high Pe. Hence, the volume dragged by a towed drop at high Pe is at least an order of magnitude smaller than the volume dragged at low Pe.

In stratified fluids, the time it takes for the partial drift to achieve a finite (zero or nonzero) asymptotic value is inversely proportional to the stratification strength ϵ_h or $Ri_h^{1/3}$. In the limit of zero stratification, the partial drift never attains a finite asymptotic value or it diverges with time, as expected in homogeneous fluids.

B. Partial drift due to an organism

Because of Eq. (18), the stream function associated with the far-field flow due to an organism (ψ_s') and a towed particle are related by

$$\psi_s' = -\frac{b}{F}\frac{\partial}{\partial r_3}\psi'. \tag{35}$$

Hence, this stream function evaluated at the edge of the marked fluid disk is given by

$$\psi_{s*}' = -\frac{b}{F}\frac{\partial \psi'}{\partial r_3}\bigg|_{(r_3=-h\tau, R=h)} = \frac{b}{hF}\frac{d\psi_*'}{d\tau}. \tag{36}$$

Substituting for ψ_{s*}' from the above equation in Eq. (31) and using the three arguments mentioned there, we get

$$D_p = 2\pi b\left(\frac{\psi_*'(\tau) - \psi_*'(\tau_0)}{F}\right). \tag{37}$$

This equation was derived earlier in the homogeneous fluids [30] but thanks to the Boussinesq approximation, it is also

valid in the stratified fluids. We rewrite ψ' in terms of $\bar{\psi}'$, express $\bar{\psi}'$ in terms of $\hat{\bar{\psi}}'$ through the inverse Fourier transform written in cylindrical coordinates and integrate first in the azimuthal direction to derive the following expression for D_p:

$$D_p = \frac{b}{2\pi\xi}\int_{-\infty}^{\infty}dk_3\int_0^{\infty}dk_r\frac{\hat{\bar{\psi}}'(k_r, k_3)}{F}e^{-ik_3\xi_h\tau}k_rJ_0(k_r\xi_h)\bigg|_{\tau_0}^{\tau}, \tag{38}$$

where $f(\tau)|_{\tau_0}^{\tau} = f(\tau) - f(\tau_0)$. Using $\tau_0 \to -\infty$, we plot the variation of D_p with τ, ϵ_h or $Ri_h^{1/3}$ at low and high Pe in Fig. 5. From this figure, we can find D_p for any initial and finite time or position of the organism relative to the marked fluid, τ_0, τ_f by subtracting $D_p(\tau = \tau_0)$ from $D_p(\tau = \tau_f)$ on any given curve.

Similar to a towed drop, an organism induces smaller partial drift in stratified fluids than that in homogeneous fluids. Also, as the stratification strength ϵ or Ri$^{1/3}$ increases for fixed h, the partial drift decreases. As mentioned earlier, these are the consequences of the stratification effect on the flow field, which causes a rapid decay of flow as well as the closed streamline flow, and both these effects reduce the drift.

Similar to that in the homogeneous fluid, at low Pe in the stratified fluid, the far-field flow due to an organism is fore-aft mirror symmetric (see Fig. 5 in Ref. [15]). Hence, the downstream drift is equal to the negative of the upstream drift. This means that zero drift is induced by any organism that travels symmetrically with respect to the initially marked fluid, starting and stopping before reorienting at equal distances from the initially marked fluid ($\tau_o = -\tau_f$). This is because the organism undergoing such motion makes the marked fluid elements move in closed-loop paths. Hence, at low Pe, any organism that exhibits most asymmetric
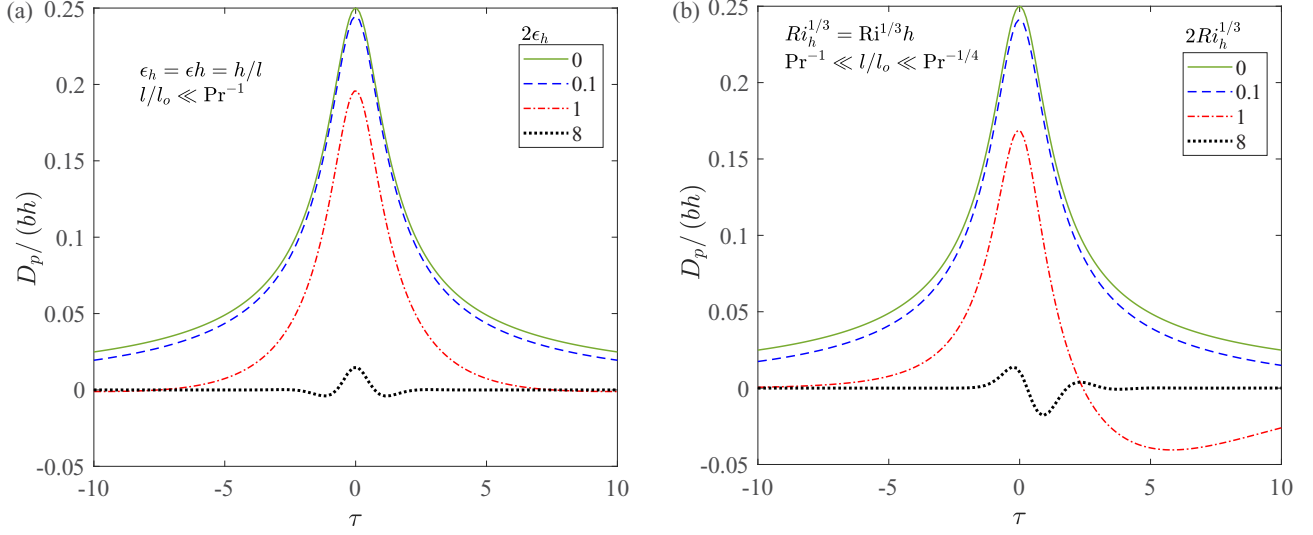
FIG. 5. The variation of the normalized partial drift induced by a swimming organism D_p/bh with (a) τ, ϵ_h at low Pe and (b) $Ri_h^{1/3}$ at high Pe. Here, we choose $\tau_0 \to -\infty$. To find D_p for any value of τ_0, τ_f, subtract $D_p(\tau_0)$ from $D_p(\tau_f)$ on any specific curve.

paths with respect to the marked fluid induces the maximum partial drift $D_{p,\text{max}}$. Because the most asymmetric path corresponds to the swimmer starting right behind the marked fluid ($\tau_0 \to 0$) and stopping far ahead ($\tau_f \gg 1$) or starting far behind ($-\tau_0 \gg 1$) and stopping right after crossing the marked fluid ($\tau_f \to 0$), the maximum partial drift in stratified fluids at low Pe is given by $D_{p,\text{max}} = D_p(-\tau_0 \gg 1, \tau_f = 0) = -D_p(\tau_0 = 0, \tau_f \gg 1)$. $D_{p,\text{max}}$ in homogeneous fluids is $bh/4$. As the stratification reduces the drift, $D_{p,\text{max}}$ in stratified fluids at low Pe is less than $bh/4$ and is a decreasing function of ϵ_h.

At high Pe, the lack of fore-aft mirror symmetry means that the drift does not vanish for any symmetric travel paths of the organism. The nonmonotonic variation of D_p in the downstream [see red or black curve in Fig. 5(b)] is due to the flow reversal with respect to the usual downward flow for a pusher near $\bar{r}_3 \approx -3$ [see Fig. 2(a)]. Even though such flow reversal exists at low Pe [see Fig. 5(b) in Ref. [15]], the magnitude of the reverse flow as well as the extent of the reverse flow at low Pe is not as large as that at high Pe, due to which D_p in the downstream at low Pe exhibits no nonmonotonic trends [see Fig. 5(a)].

Because the integral in Eq. (38) is $O(1)$, in general D_p in stratified fluids is $O(b/\xi)$, where $\xi = \epsilon$, $Ri^{1/3}$ at low and high Pe, respectively. As long as $b \geqslant O(1)$ and a swimmer at low Pe does not travel symmetrically with respect to the marked fluid, $D_p \gg 1$ because $\xi \ll 1$ in our analysis. Hence, a swimmer in stratified fluids displaces a volume of fluid that is much larger than its own.

As mentioned earlier, the error in finding D_p comes from neglecting the deflection of streamlines at the edge of the marked fluid with respect to the free stream position, neglecting the bracketed term in Eq. (31) and neglecting the near-field flow contribution to the drift. The error from these three sources is $O(1)$ for a swimming organism. Because $D_p \gg 1$ unless $b \ll 1$ or the swimmer travels symmetrically relative to the marked fluid at low Pe, this error can be neglected.

We note that the only theoretical calculation of the mixing efficiency of swimming organisms in a stratified fluid at neg-

ligible inertia and weak stratification was done for point-sized swimmers [16], whereas the partial drift found here is valid for finite-sized organisms. Naively, we compare these two estimates at low Pe and find that, while the mixing efficiency is $O(\epsilon^3) \ll 1$, the dimensionless partial drift is $O(b/\epsilon) \gg 1$ unless the stresslet strength $b \ll 1$. A consistent comparison of these two estimates requires the calculation of the mixing efficiency of the finite-sized organisms. Unlike the drift or partial drift, the mixing efficiency of the finite-sized organisms depends solely on the near-field variables (see the following discussion) and hence its calculation is beyond the scope of the present paper because we focus on the derivation, analysis, and application of the far-field flow.

We show here why the mixing efficiency of a finite-sized organism depends only on the near-field variables. As mentioned in the introduction, the mixing efficiency is the ratio of the rate of creation of gravitational potential energy to the rate of work done on the fluid and is precisely given by the following expression:

$$\text{Ri} \frac{\int \rho' w_3' dV}{\int \mathbf{n} \cdot \boldsymbol{\sigma}' \cdot \mathbf{w}' dS} \sim \text{Ri} \int \rho' w_3' dV. \tag{39}$$

Here $\boldsymbol{\sigma}'$ is the stress associated with the disturbance flow $\mathbf{w}'$, the volume integral should be evaluated over the entire fluid domain while the surface integral should be evaluated on the swimmer's surface. Because $\mathbf{w}' \approx O(1)$ and $\boldsymbol{\sigma}' \sim \nabla \mathbf{w}' \approx O(1)$ on the swimmer's surface, we can estimate the surface integral to be $O(1)$. At low Pe, the flow and the density disturbance far away from the organism decay rapidly with the position (see Ref. [15]). At high Pe, we showed in this paper that the far-field disturbance flow again decays rapidly with position. At high Pe, ρ' far from an organism is governed by $\mathbf{u} \cdot \nabla \rho' = -w_3' = -\frac{b}{F} \frac{\partial}{\partial r_3}$ (the far-field vertical velocity due to a towed particle). This means that, at high Pe, the far-field density disturbance due to an organism scales as the far-field vertical velocity due to a towed particle that also decays rapidly with position. Hence, at both low and high Pe, ρ', w_3'

far from the organism decay rapidly with position. This means that the far-field region does not contribute to the integral and the mixing efficiency depends only on the near-field variables.

IV. CONCLUSIONS

In this work, we derived the far-field flow due to a towed particle and a neutrally buoyant swimming organism in a linearly density stratified fluid in the limits of low Re, Ri, and high Pe. Here, the Reynolds number Re is the ratio of the inertia to the viscous forces, the viscous Richardson number Ri is the ratio of the buoyancy to the viscous forces, and the Péclet number Pe is the ratio of the advection to the diffusion of the density. Our work complements the similar calculation done in the limit of low Re, Ri, Pe to find the flow due to a point-force and force-dipole in a stratified fluid [15], which in the limit considered is the same as the far-field flow due to a towed particle and a neutrally buoyant swimming organism. Similar to that at low Pe, stratification causes the flow to decay rapidly and also makes the streamlines closed but, unlike that at low Pe, the fore-aft symmetry or mirror symmetry is destroyed at high Pe due to the advective transport of density in only one direction.

To demonstrate the application of these far-field flows at low and high Pe, we used them to derive the drift induced by a towed drop and a swimming organism. At low Pe, the drift due to a towed drop is $O(h^2 V_b) \gg O(V_b)$, while at high Pe, the induced drift is at least an order of magnitude smaller than that at low Pe. Here, h measures the extent of the marked fluid and V_b is the volume of the drop or the organism. Hence, a towed drop drags a large volume of stratified fluid as compared with its volume at low Pe but not so much at high Pe. The partial drift due to a swimming organism is $O(bV_b/\xi)$ where b is the stresslet strength and $\xi \ll 1$ is the stratification strength characterized by $\epsilon = (\text{RiPe})^{1/4}, \text{Ri}^{1/3}$ at low and high Pe, respectively. Interestingly, the partial drift induced by a swimmer in a homogeneous fluid at finite Re is also of the similar form $O(bV_b/\text{Re})$. Hence, unless a swimmer exerts a low stresslet ($b \ll 1$), it displaces a large volume of stratified fluid relative to its own volume.

There are certainly two avenues for future research. To generalize the validity of our calculation to large swimming organisms like crustaceans ($1 \leqslant \text{Re} \leqslant 1000$), where inertia is not negligible, it is necessary to consider the simultaneous influence of inertia and stratification. Usually, the gait of a swimming organism is unsteady and time-periodic, unlike the steady gait considered in this work. In homogeneous fluids, at finite Re, it was shown that the drift induced by a steady swimmer is the same as the time-averaged drift due to an unsteady swimmer [30]. It would be interesting to explore such correlations between the drift induced by steady and unsteady swimmers in stratified fluids.

APPENDIX: RELATION BETWEEN THE FLOW FIELD AND THE STREAM FUNCTION IN THE FOURIER SPACE

In the cylindrical coordinates whose origin is at the center of the particle or the organism, the flow in the radial direction is related to the stream function via

$$\bar{w}'_\zeta = -\frac{1}{\bar{\zeta}} \frac{\partial \bar{\psi}'}{\partial \bar{z}}, \tag{A1}$$

where $\bar{\zeta} = \frac{\bar{r}_1}{\cos \phi} = \frac{\bar{r}_2}{\sin \phi}$ is the rescaled radial coordinate in the cylindrical coordinate system while ϕ is the azimuthal angle. We express $\bar{w}'_\zeta$ in terms of $\bar{w}'_1$ and $\bar{w}'_2$ through $\bar{w}'_\zeta = \bar{w}'_1 \cos \phi + \bar{w}'_2 \sin \phi$ and simplify the above equation to obtain

$$\bar{r}_1 \bar{w}'_1 + \bar{r}_2 \bar{w}'_2 = -\frac{\partial \bar{\psi}'}{\partial \bar{z}}. \tag{A2}$$

Noting that the Fourier transform of $\frac{\partial \bar{\psi}'}{\partial \bar{z}}$, $\bar{r}_1 \bar{w}'_1$, and $\bar{r}_2 \bar{w}'_2$ are respectively $ik_3 \hat{\bar{\psi}}'$, $i\frac{\partial \hat{\bar{w}}'_1}{\partial k_1}$, and $i\frac{\partial \hat{\bar{w}}'_2}{\partial k_2}$, we take the Fourier transform of the above equation to derive

$$i\frac{\partial \hat{\bar{w}}'_1}{\partial k_1} + i\frac{\partial \hat{\bar{w}}'_2}{\partial k_2} = -ik_3 \hat{\bar{\psi}}'. \tag{A3}$$

Solving for $\hat{\bar{\psi}}'$ then gives Eq. (32).

[1] A. M. Ardekani, A. Doostmohammadi, and N. Desai, Transport of particles, drops, and small organisms in density stratified fluids, Phys. Rev. Fluids **2**, 100503 (2017).

[2] J. Magnaudet and M. J. Mercier, Particles, drops, and bubbles moving across sharp interfaces and stratified layers, Annu. Rev. Fluid Mech. **52**, 61 (2020).

[3] K. Kindler, A. Khalili, and R. Stocker, Diffusion-limited retention of porous particles at density interfaces, Proc. Natl. Acad. Sci. U. S. A. **107**, 22163 (2010).

[4] A. Doostmohammadi and A. M. Ardekani, Suspension of solid particles in a density stratified fluid, Phys. Fluids **27**, 023302 (2015).

[5] S. Dabiri, A. Doostmohammadi, M. Bayareh, and A. Ardekani, Rising motion of a swarm of drops in a linearly stratified fluid, Int. J. Multiphase Flow **69**, 8 (2015).

[6] R. Dandekar, V. A. Shaik, and A. M. Ardekani, Motion of an arbitrarily shaped particle in a density stratified fluid, J. Fluid Mech. **890**, A16 (2020).

[7] B. Bergström and J.-O. Strömberg, Behavioural differences in relation to pycnoclines during vertical migration of the euphausiids *Meganyctiphanes norvegica* (M. Sars) and *Thysanoessa raschii* (M. Sars), J. Plankton Res. **19**, 255 (1997).

[8] T. Jephson and P. Carlsson, Species- and stratification-dependent diel vertical migration behaviour of three dinoflagellate species in a laboratory study, J. Plankton Res. **31**, 1353 (2009).

[9] A. Doostmohammadi, R. Stocker, and A. M. Ardekani, Low-Reynolds-number swimming at pycnoclines, Proc. Natl. Acad. Sci. U. S. A. **109**, 3856 (2012).

[10] R. Dandekar, V. A. Shaik, and A. M. Ardekani, Swimming sheet in a density-stratified fluid, J. Fluid Mech. **874**, 210 (2019).

[11] B. S. Sherman, I. T. Webster, G. J. Jones, and R. L. Oliver, Transitions between Auhcoseira and Anabaena dominance in a turbid river weir pool, Limnol. Oceanogr. **43**, 1902 (1998).

[12] E. Kunze, Biologically generated mixing in the ocean, Annu. Rev. Mar. Sci. **11**, 215 (2019).

[13] A. M. Leshansky and L. M. Pismen, Do small swimmers mix the ocean? Phys. Rev. E **82**, 025301(R) (2010).

[14] G. Subramanian, Viscosity-enhanced bio-mixing of the oceans, Curr. Sci. **98**, 1103 (2010).

[15] A. M. Ardekani and R. Stocker, Stratlets: Low Reynolds Number Point-Force Solutions in a Stratified Fluid, Phys. Rev. Lett. **105**, 084502 (2010).

[16] G. L. Wagner, W. R. Young, and E. Lauga, Mixing by microorganisms in stratified fluids, J. Mar. Res. **72**, 47 (2014).

[17] V. A. Shaik and A. M. Ardekani, Drag, deformation, and drift volume associated with a drop rising in a density stratified fluid, Phys. Rev. Fluids **5**, 013604 (2020).

[18] K. Katija and J. O. Dabiri, A viscosity-enhanced mechanism for biogenic ocean mixing, Nature (London) **460**, 624 (2009).

[19] K. Katija, Biogenic inputs to ocean mixing, J. Exp. Biol. **215**, 1040 (2012).

[20] Y. Zvirin and R. Chadwick, Settling of an axially symmetric body in a viscous stratified fluid, Int. J. Multiphase Flow **1**, 743 (1975).

[21] S. Wang and A. M. Ardekani, Biogenic mixing induced by intermediate Reynolds number swimming in stratified fluids, Sci. Rep. **5**, 17448 (2015).

[22] R. More and A. M. Ardekani, Motion of an inertial squirmer in a density stratified fluid, J. Fluid Mech. **905**, A9 (2020).

[23] E. J. List, Laminar momentum jets in a stratified fluid, J. Fluid Mech. **45**, 561 (1971).

[24] G. S. Janowitz, On wakes in stratified fluids, J. Fluid Mech. **33**, 417 (1968).

[25] J. Zhang, M. J. Mercier, and J. Magnaudet, Core mechanisms of drag enhancement on bodies settling in a stratified fluid, J. Fluid Mech. **875**, 622 (2019).

[26] L. G. Leal, *Advanced Transport Phenomena* (Cambridge University Press, Cambridge, 2007).

[27] D. D. Gray and A. Giorgini, The validity of the Boussinesq approximation for liquids and gases, Int. J. Heat Mass Transfer **19**, 545 (1976).

[28] K. Y. Yick, C. R. Torres, T. Peacock, and R. Stocker, Enhanced drag of a sphere settling in a stratified fluid at small Reynolds numbers, J. Fluid Mech. **632**, 49 (2009).

[29] J. Happel and H. Brenner, *Low Reynolds Number Hydrodynamics*, Mechanics of Fluids and Transport Processes (Springer Netherlands, Dordrecht, 1981), Vol. 1.

[30] N. G. Chisholm and A. S. Khair, Partial drift volume due to a self-propelled swimmer, Phys. Rev. Fluids **3**, 014501 (2018).

[31] F. Candelier, R. Mehaddi, and O. Vauquelin, The history force on a small particle in a linearly stratified fluid, J. Fluid Mech. **749**, 184 (2014).

[32] R. Mehaddi, F. Candelier, and B. Mehlig, Inertial drag on a sphere settling in a stratified fluid, J. Fluid Mech. **855**, 1074 (2018).

[33] H. Lee, I. Fouxon, and C. Lee, Sedimentation of a small sphere in stratified fluid, Phys. Rev. Fluids **4**, 104101 (2019).

[34] D. G. Voelz, *Computational Fourier Optics: A MATLAB Tutorial* (SPIE, Bellingham, WA, 2011).

[35] J. R. Blake, A note on the image system for a stokeslet in a no-slip boundary, Math. Proc. Cambridge Philos. Soc. **70**, 303 (1971).

[36] J. R. Blake and A. T. Chwang, Fundamental singularities of viscous flow, J. Eng. Math. **8**, 23 (1974).

[37] I. Eames, D. Gobby, and S. B. Dalziel, Fluid displacement by Stokes flow past a spherical droplet, J. Fluid Mech. **485**, 67 (2003).

[38] N. G. Chisholm and A. S. Khair, Drift volume in viscous flows, Phys. Rev. Fluids **2**, 064101 (2017).